

**Fracture and Creep of an  $\text{Al}_2\text{O}_3$ – $\text{SiC}$  (whisker)– $\text{TiC}$  (particle) Composite**

A. R. DE ARELLANO–LÓPEZ

Dept. de Fisica de la Materia Condensada

Universidad de Sevilla, P.O. Box 1065, 41080 Sevilla (Spain)

B. I. SMIRNOV

A. F. Ioffe Physico–Technical Institute

Russian Academy of Sciences, 194021 St. Petersburg (Russia)

J. J. SCHULDIES

Industrial Ceramic Technology

Ann Arbor, Michigan 48103 (U.S.A.)

E. T. PARK, K. C. GORETTA, J. L. ROUTBORT

Energy Technology Division, Argonne National Laboratory

Argonne, Illinois 60439 (U.S.A.)

February 1998

RECEIVED

SEP 21 1999

OST

The submitted manuscript has been created by the University of Chicago as Operator of Argonne National Laboratory ("Argonne") under Contract No. W-31-109-ENG-38 with the U.S. Department of Energy. The U.S. Government retains for itself, and others acting on its behalf, a paid-up, nonexclusive, irrevocable worldwide license in said article to reproduce, prepare derivative works, distribute copies to the public, and perform publicly and display publicly, by or on behalf of the Government.

Submitted to Proceedings of 6th International Conference of the Science of Hard Materials, March 9–14, 1998, Lanzarote, Spain.

\*This work was supported by the North Atlantic Treaty Organization, under Grant HIGH TECHNOLOGY CRG/No. 960793; the Ministerio de Educación y Ciencias of Spain, under CICYT Project MAT94-0481; and the U.S. Department of Energy, Energy Research Laboratory Technology Transfer Program, under Contract W-31-109-Eng-38.

## **DISCLAIMER**

This report was prepared as an account of work sponsored by an agency of the United States Government. Neither the United States Government nor any agency thereof, nor any of their employees, make any warranty, express or implied, or assumes any legal liability or responsibility for the accuracy, completeness, or usefulness of any information, apparatus, product, or process disclosed, or represents that its use would not infringe privately owned rights. Reference herein to any specific commercial product, process, or service by trade name, trademark, manufacturer, or otherwise does not necessarily constitute or imply its endorsement, recommendation, or favoring by the United States Government or any agency thereof. The views and opinions of authors expressed herein do not necessarily state or reflect those of the United States Government or any agency thereof.

## **DISCLAIMER**

**Portions of this document may be illegible  
in electronic image products. Images are  
produced from the best available original  
document.**

# Fracture and Creep of an $\text{Al}_2\text{O}_3$ – $\text{SiC}$ (whisker)– $\text{TiC}$ (particle) Composite

A. R. DE ARELLANO–LÓPEZ

Dept. de Fisica de la Materia Condensada

Universidad de Sevilla, P.O. Box 1065, 41080 Sevilla (Spain)

B. I. SMIRNOV

A. F. Ioffe Physico–Technical Institute

Russian Academy of Sciences, 194021 St. Petersburg (Russia)

J. J. SCHULDIES

Industrial Ceramic Technology

Ann Arbor, Michigan 48103 (U.S.A.)

E. T. PARK, K. C. GORETTA, J. L. ROUTBORT

Energy Technology Division, Argonne National Laboratory

Argonne, Illinois 60439 (U.S.A.)

## Abstract

High-temperature fracture strength and compressive creep of an electrodischarge-machinable composite,  $\text{Al}_2\text{O}_3$ –30.9 vol.%  $\text{SiC}$  whiskers–23 vol.%  $\text{TiC}$  particles have been studied to  $1200^\circ\text{C}$  and  $1450^\circ\text{C}$ , respectively, in inert atmosphere. Microstructures of fractured and deformed specimens were examined by scanning and transmission electron microscopy. Fast fracture occurred at  $T \leq 1200^\circ\text{C}$ . Steady-state creep was achieved for  $T > 1350^\circ\text{C}$  at

stresses  $< 80$  MPa, with the rate-controlling mechanism being partially unaccommodated grain-boundary sliding, with a stress exponent of  $\approx 1$  and an activation energy of  $\approx 470$  kJ/mol.

## 1. Introduction

Significant improvements in strength, toughness, and creep resistance of ceramic materials have been achieved in the past decade. This is particularly true for ceramic-matrix composites [1], for which SiC-whisker-reinforced  $\text{Al}_2\text{O}_3$ -based composites have become a classic system and the object of extensive study [2-5]. High machining costs for complex parts have limited use of these composites and, therefore, they have not found wide-spread application despite their uniquely favorable properties, such as low density, chemical and thermal stability, and mechanical durability. A composite has recently been developed with sufficiently high electrical conductivity to take a step towards the possible realization of the goal of wider commercial usage. TiC particles are added to  $\text{Al}_2\text{O}_3$  powder and SiC whiskers to produce an electrodischarge-machinable ceramic composite [6]. These composites are semimetals with high electrical conductivity [7,8].

Laboratories in Spain, Russia, and the U.S.A., under the auspices of NATO, have extensively characterized the microstructural and mechanical properties of this new ceramic composite with a goal of determining processing paths and microstructures that will yield conducting composites with further improved mechanical properties. Previous work on  $\text{Al}_2\text{O}_3$ -SiC (whisker)-TiC (particle) composites (AlSiTi) dealt with microstructure and room-temperature mechanical properties, such as fracture strength, fracture

toughness, microhardness, elastic modulus, and response to solid-particle erosion [8,9]. Summarizing the earlier findings: AlSiTi has an elastic modulus at room temperature of 410 GPa, microhardness values of 9.6–20 GPa (depending on whether the indentor was centered on a TiC particle or not), and an indentation fracture toughness ( $K_{IC}$ ) of  $9.6 \text{ MPa(m)}^{0.5}$ . Microcracking is thought to be the most important toughening mechanism operating in this composite. Three and four-point bending strengths of AlSiTi were 825 and 680 MPa, respectively. Tensile surfaces were, however, not polished. High-temperature compressive creep of this composite has been investigated at 1350–1450°C in inert atmospheres [10]. The creep resistance is good and, at lower stresses, deformation occurs by partially unaccommodated grain-boundary sliding.

High-temperature mechanical properties play an important role in development and implementation of practical applications of ceramic composites because many of the potential applications are at elevated temperatures. Therefore, this work is aimed at measuring the high-temperature fracture strength and creep response of an AlSiTi composite. Additionally, the elastic modulus was measured to 1000°C.

## 2. Experiments

A commercial composite (CRYSTALOY 2311EDX) fabricated by hot-pressing at 1700–1800°C a mixture of 30.9 vol.% SiC whiskers, 23.0 vol.% TiC powder, and balance  $\text{Al}_2\text{O}_3$  was examined [6]. Optical micrographs of the SiC whiskers and a surface polished perpendicular to the hot-pressing direction are shown in Fig. 1. The material is ≈99% dense. Comparison of the initial (Fig. 1a) and

final whisker lengths (Fig. 1b) indicated that considerable damage to the SiC whisker occurred during processing. X-ray diffraction indicated strong TiC and Al<sub>2</sub>O<sub>3</sub> peaks and weaker SiC peaks.

Bend-bar samples 2.5 x 3.8 x 38 mm or 2.5 x 3.0 x 38 mm were cut with a slow-speed diamond saw. Bar edges were chamfered and each tensile surface was ground with 1- $\mu$ m diamond paste. Strength tests were performed at a crosshead velocity of  $\approx$ 1.3 mm/min in an Instron Model 1125 [11]. Room-temperature tests were conducted in air with steel tooling, inner load span of 9.5 mm, outer load span of 23.8 mm. High-temperatures tests were conducted in Ar with Al<sub>2</sub>O<sub>3</sub>-SiC whisker tooling [5], inner load span of 9.9 mm, outer load span 17.6 mm. The elastic modulus was measured by a resonance frequency method [12].

For creep, parallelepipeds  $\approx$ 5 x 2 x 2 mm were cut and the compression surfaces were polished to be flat and parallel. Specimens were deformed at 1350–1450°C under uniaxial compression in the direction of the longer axis. The low-stress range was studied in Ar with a constant-load (CL) creep apparatus [13]; higher stresses and strain rates were studied in high-purity N<sub>2</sub> at approximately constant strain rate (CSR) [11].

Microstructural features of both undeformed and deformed specimens were examined by X-ray diffraction, scanning electron microscopy (SEM), and transmission electron microscopy (TEM). SEM samples were prepared by polishing the composite to a 1- $\mu$ m finish and coating with carbon. TEM foils were prepared by grinding, dimpling, and ion-milling. Preparation of TEM

foils was complicated because the TiC particles proved to be very difficult to thin by ion-milling. TEM results have been described [10].

### **3. Results and Discussion**

#### **3.1. Elastic Modulus**

Variation of Young's modulus (E) with temperature is shown in Fig. 2. The value of E at room temperature for the composite was approximately 2.5% higher than E for pure  $\text{Al}_2\text{O}_3$  [14]. The value of  $1/E$  ( $dE/dT$ ) from 25 to  $1000^\circ\text{C}$  was  $8.5 \times 10^{-5} \text{ }^\circ\text{C}^{-1}$ , almost equal to the value of  $8.3 \times 10^{-5} \text{ }^\circ\text{C}^{-1}$  found for  $\text{Al}_2\text{O}_3$  in the same temperature range [14]. The SiC and TiC additions, therefore, seem to have had little effect on E.

#### **3.2. Fracture Strength**

Fracture strength is plotted as a function of temperature in Fig. 3. The strength of 440 MPa measured at room temperature is considerably lower than that reported previously [9]. Fractures originated at processing flaws. The discrepancy between these measurements performed on polished samples and our previous measurements must reflect variability in processing or sample preparation and will require further investigation. Strength was virtually independent of temperature to  $1000^\circ\text{C}$ , but decreased slightly at  $1200^\circ\text{C}$ , which is probably the limit of practical use of this material because creep could be excessive at higher temperatures. Surfaces of samples fractured at room temperature (Fig. 4a) and  $1200^\circ\text{C}$  (Fig. 4b) indicate that fracture was a combination of intergranular and transgranular.

### 3.3. Creep

A standard creep equation [15] was used to analyze the results:

$$\dot{\varepsilon} = A\sigma^n \exp(-Q/RT), \quad (1)$$

where  $\dot{\varepsilon}$  is the strain rate,  $\sigma$  is the stress, R and T have their usual meanings, and A is constant. The parameters n, the stress exponent, and Q, the activation energy, are related to plastic deformation mechanisms through various models [13,15].

Figure 5 shows a log-log plot of strain rate vs. stress for five different samples. At 1400°C, the maximum stress in the CL tests was  $\approx$ 80 MPa; stresses in the CSR tests were 150–540 MPa. The low-stress regime ( $< 80$  MPa) can be characterized by a stress exponent  $\approx 1.0 \pm 0.3$ , which is typical for diffusional creep of monolithic fine-grained polycrystalline ceramics [16]. On the other hand, the high-stress regime showed an important degree of sample to sample variability, due to the formation of macroscopic damage [10]. The activation energy was determined to be  $\approx 470$  kJ/mole at 23 MPa and 1350–1450°C.

SEM and TEM revealed that cavitation occurred, especially at the higher stresses. Little dislocation activity was observed in TEM in the samples before or after deformation [10]. The TiC particles appeared to remain intact throughout the plastic deformation process and can therefore be considered as rigid inclusions.

A stress exponent of  $\approx 1$  for lower stresses, microstructural observations that cavities formed during plastic deformation, and absence of dislocation activity can be related to a mechanism that involves grain-boundary sliding, but for which the sliding was not fully accommodated by diffusion [17]. Creep resistance for the AlSiTi composite might be improved by inhibiting grain-boundary sliding, which could be achieved by adding more of a rigid reinforcing phase or by preserving more of the initial SiC whisker length.

The creep resistance of the AlSiTi composite is comparable to that of other whisker-reinforced ceramic composites with similar grain size ( $\text{Al}_2\text{O}_3$  grain size  $\approx 1 \mu\text{m}$ ). A comparison with creep of  $\text{Al}_2\text{O}_3$ -30 vol.% SiC whisker [18] and a  $\text{Al}_2\text{O}_3$ -5.5 vol.%  $\text{ZrO}_2$  particle-28 vol.% SiC whisker [19] composites is shown in Fig. 6. At lower stresses, in the  $n \approx 1$  region, all composites creep at about the same rate, whereas the AlSiTi shows more creep resistance and damage tolerance at the higher stresses.

#### 4. Summary

The strength of an  $\text{Al}_2\text{O}_3$ -30.9 vol.% SiC (whiskers)-23 vol.% TiC (particles) was independent of temperature to  $1000^\circ\text{C}$ , but decreased slightly at  $1200^\circ\text{C}$ . The fracture mode, a combination of transgranular and intergranular, was unaffected by temperature. At temperatures  $> 1350^\circ\text{C}$ , steady-state creep was achieved. At stresses below 80 MPa, creep occurred by partially unaccommodated grain-boundary sliding, with a stress exponent of  $\approx 1$  and an activation energy of  $\approx 470 \text{ kJ/mole}$ .

## **Acknowledgments**

This work was supported by the North Atlantic Treaty Organization, under Grant HIGH TECHNOLOGY CRG/No. 960793; the Ministerio de Educación y Ciencias of Spain, under CICYT Project MAT94-0481; and the U.S. Department of Energy, Energy Research Laboratory Technology Transfer Program, under Contract W-31-109-Eng-38.

## References

1. A. G. Evans and D. B. Marshall, *Acta Metall.*, 37 (1989) 2567.
2. H.-T. Lin and P. F. Becher, *J. Am. Ceram. Soc.*, 73 (1990) 1378.
3. J. P. Singh, K. C. Goretta, J. L. Routbort, D. S. Kupperman, and J. F. Rhodes, *Adv. Ceram. Mater.*, 3 (1988) 357.
4. E. S. Fisher, M. H. Manghnani, J.-F. Wang, and J. L. Routbort, *J. Am. Ceram. Soc.* 75 (1992) 908.
5. A. R. de Arellano-López, A. Domínguez-Rodríguez, K. C. Goretta, and J. L. Routbort, *J. Am. Ceram. Soc.*, 76 (1993) 1425.
6. J. J. Schuldies, *EDM Today*, Nov./Dec. 1992, p. 16.
7. B. I. Smirnov, Russian Academy of Sciences, St. Petersburg, unpublished information.
8. M. Jiang, K. C. Goretta, D. Singh, J. L. Routbort, and J. J. Schuldies, *Ceram. Eng. Sci. Proc.*, 18 (1997) 239.
9. B. I. Smirnov, V. I. Nikolaev, T. S. Orlova, V. V. Shpeizman, A. R. de Arellano-López, K. C. Goretta, D. Singh, and J. L. Routbort, *Mater. Sci. Eng. A*, in press (1998).
10. A. R. de Arellano-López, B. I. Smirnov, K. C. Goretta, and J. L. Routbort, *Mater. Sci. Eng. A*, in press (1998).
11. J. L. Routbort, *Acta Metall.*, 30 (1982) 663.
12. H. J. McSkimin, in *Physical Acoustics*, Vol. 1, Part A, ed. W. P. Mason (Academic Press, New York, 1964) p. 271.
13. H. Gervais, B. Pellisier, and J. Castaing, *Rev. Int. Hautes Temp. Refract.*, 15 (1978) 43.
14. M. Fukuhara and I. Yamauchi, *J. Mater. Sci.* 28, (1993) 4681.
15. W. R. Cannon and T. G. Langdon, *J. Mater. Sci.* 23 (1988) 1.

16. H. J. Frost and M. F. Ashby, *Deformation Mechanism Maps* (Pergamon Press, New York, 1982).
17. A. R. de Arellano-López, A. Domínguez-Rodríguez, K. C. Goretta, and J. L. Routbort, in *Plastic Deformation of Ceramics*, eds. R. C. Bradt, C. A. Brookes, and J. L. Routbort (Plenum Press, New York, 1995) p. 533.
18. A. R. de Arellano-López, F. L. Cumbre, A. Domínguez-Rodríguez, K. C. Goretta, and J. L. Routbort, *J. Am. Ceram. Soc.*, 73 (1993) 1297.
19. J. M. Calderoñ-Moreno, A.R. DeArellano-López, A. Domínguez-Rodríguez, and J. L. Routbort, *Mater. Sci. Eng. A*209 (1996) 111.

## Figure captions

Figure 1. Optical photomicrographs of (a) SiC whiskers and (b) AlSiTi composite.

Figure 2. Variation of E as a function of temperature.

Figure 3. Four-point-bend fracture strength as a function of temperature.

Figure 4. SEM photomicrographs of fracture surfaces at (a) room temperature and (b) 1200°C.

Figure 5. Creep results from five AlSiTi samples; each symbol represents a different sample.

Figure 6. Creep data at 1400°C from this work (triangles) compared with creep of  $\text{Al}_2\text{O}_3$ –30 vol.% SiC whisker (dashed line) and  $\text{Al}_2\text{O}_3$ –5.5 vol.%  $\text{ZrO}_2$  particle–28 vol.% SiC whisker (solid line) composites.

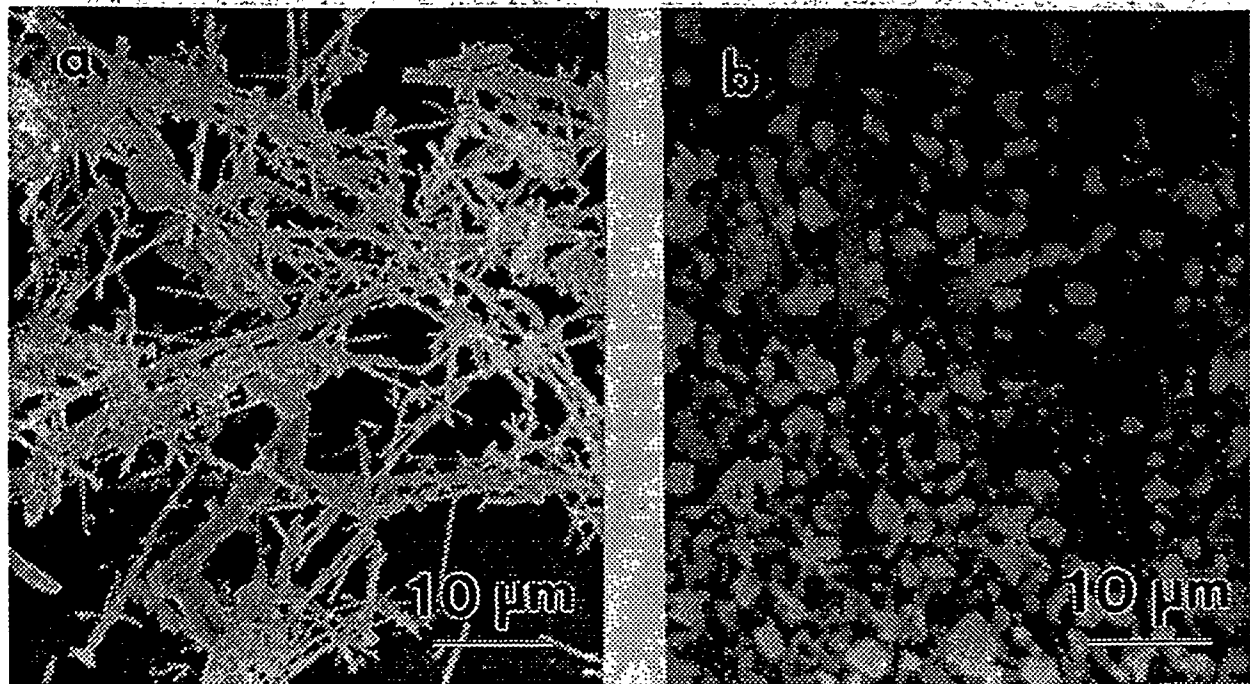


Figure 1. Optical photomicrographs of (a) SiC whiskers and (b) AlSiTi composite.

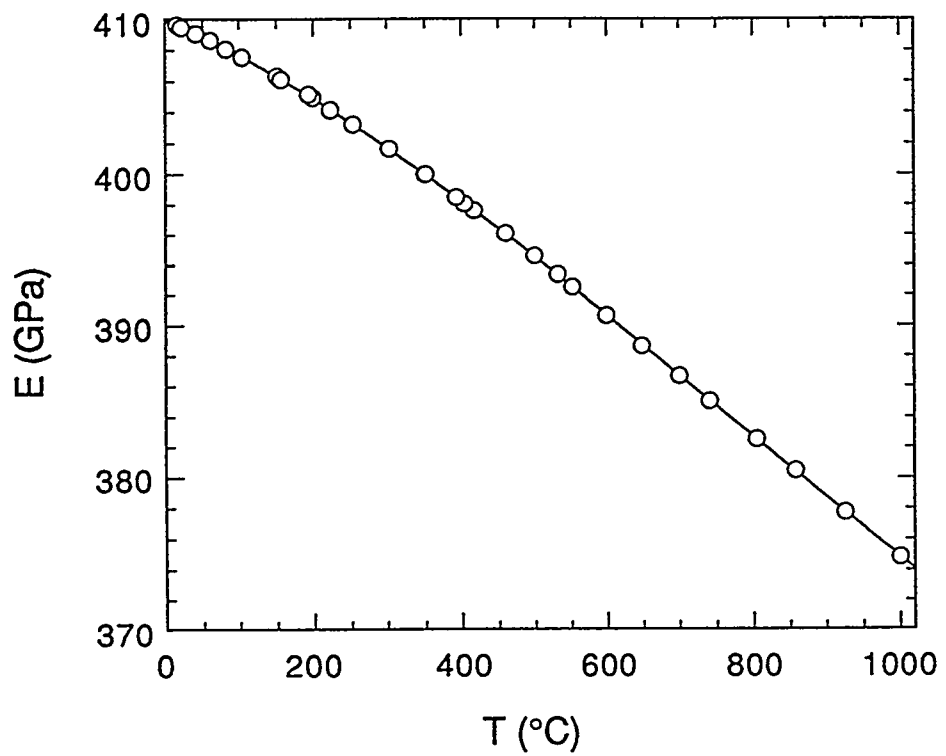


Figure 2. Variation of E as a function of temperature.

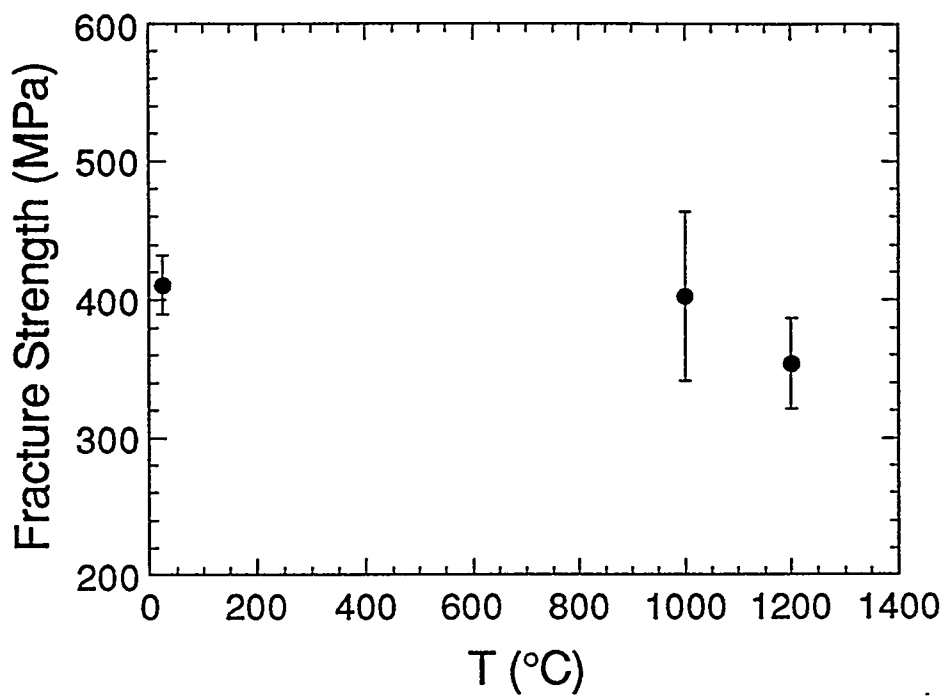


Figure 3. Four-point-bend fracture strength as a function of temperature.

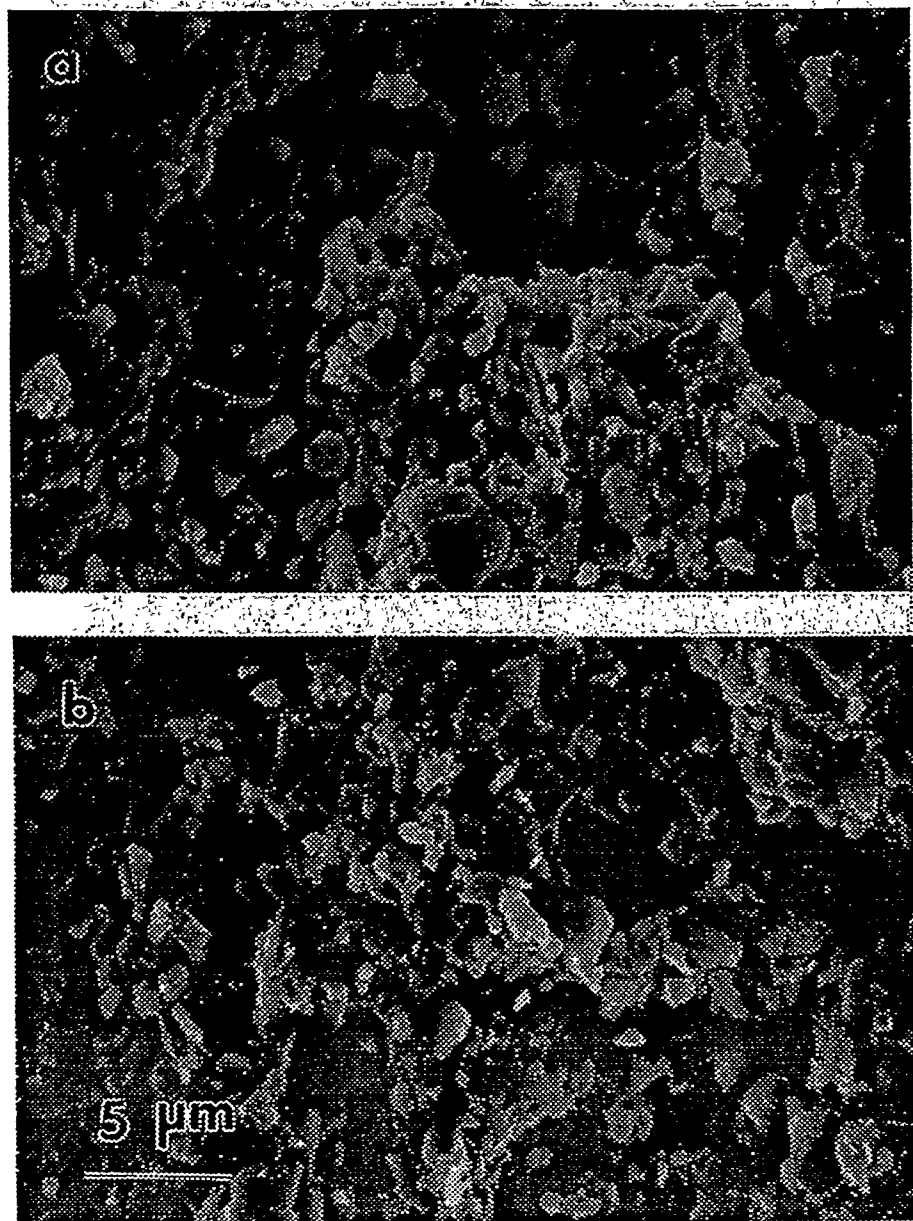


Figure 4. SEM photomicrographs of fracture surfaces at (a) room temperature and (b) 1200°C.

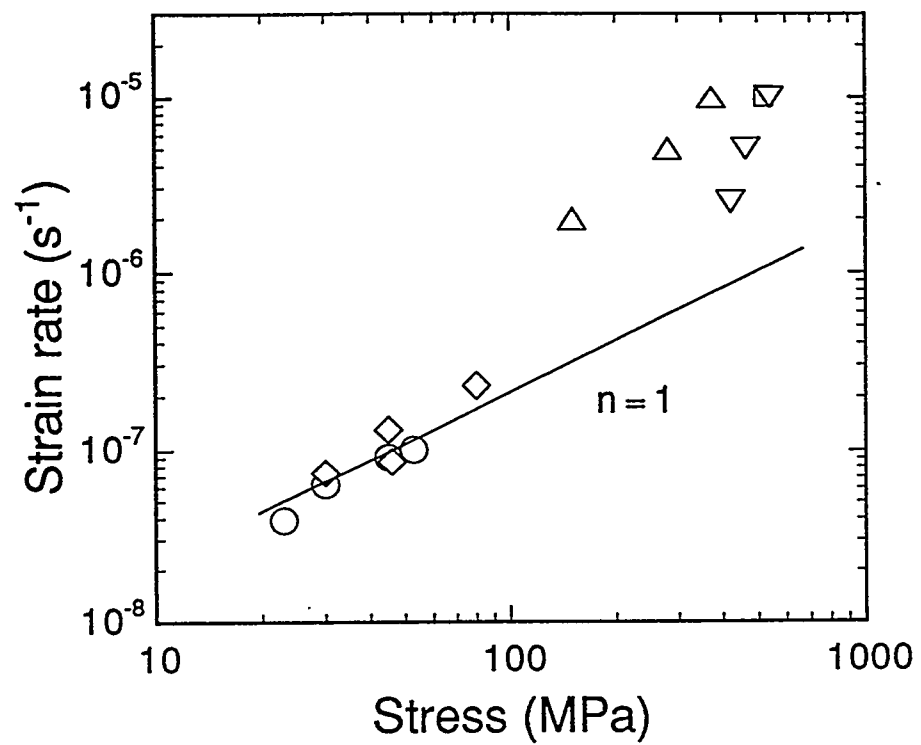


Figure 5. Creep results from five AlSiTi samples; each symbol represents a different sample.

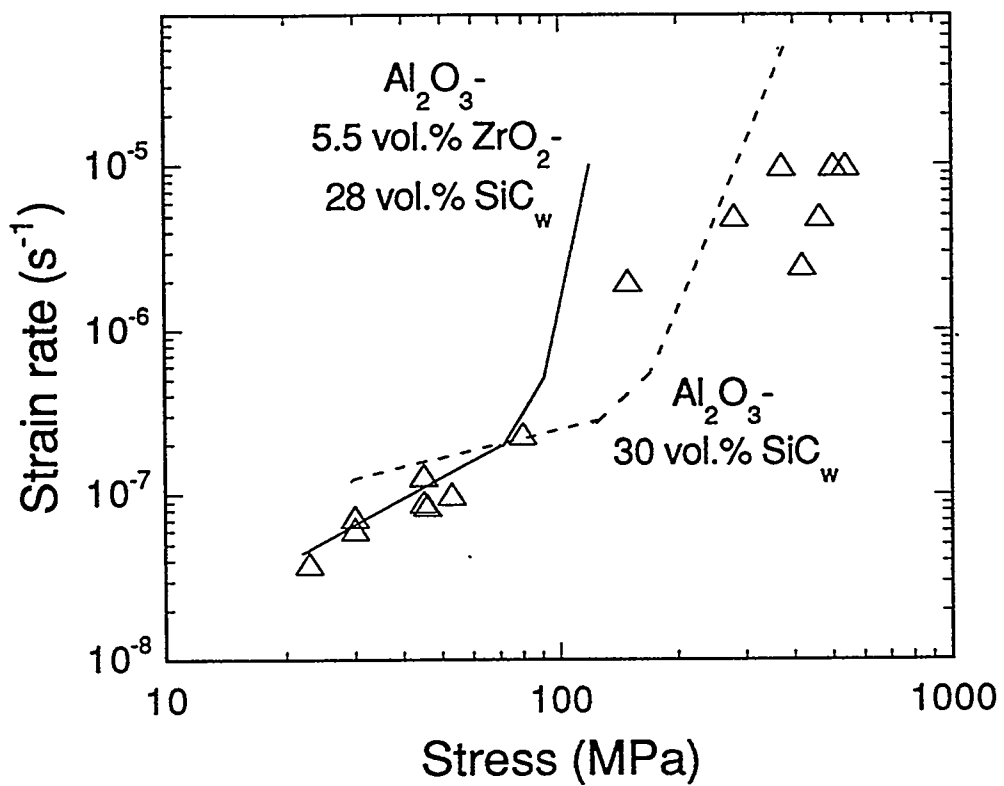


Figure 6. Creep data at 1400°C from this work (triangles) compared with creep of  $\text{Al}_2\text{O}_3$ -30 vol.% SiC whisker (dashed line) and  $\text{Al}_2\text{O}_3$ -5.5 vol.%  $\text{ZrO}_2$  particle-28 vol.% SiC whisker (solid line) composites.